A test of spatial temporal decoding mechanisms in the superior colliculus

Husam A. Katnani, A. J. Van Opstal and Neeraj J. Gandhi

J Neurophysiol 107:2442-2452, 2012. First published 25 January 2012; doi:10.1152/jn.00992.2011

Journal of Neurophysiology publishes original articles on the function of the nervous system. It is published 12 times a year (monthly) by the American Physiological Society, 9650 Rockville Pike, Bethesda MD 20814-3991. ISSN: 0022-3077, ESSN: 1522-1598. Visit our website at http://www.the-aps.org/.

J Neurophysiol 107: 2442–2452, 2012.
First published January 25, 2012; doi:10.1152/jn.00992.2011.

A test of spatial temporal decoding mechanisms in the superior colliculus

Husam A. Katnani,[1,4] A. J. Van Opstal,[5] and Neeraj J. Gandhi[1,2,3,4]

Departments of [1]Bioengineering, [2]Otolaryngology, and [3]Neuroscience and [4]Center for Neural Basis of Cognition, University of Pittsburgh, Pittsburgh, Pennsylvania; and [5]Department of Biophysics, Donders Institute for Brain, Cognition, and Behavior, Radboud University Nijmegen, Nijmegen, The Netherlands

Submitted 28 October 2011; accepted in final form 23 January 2012

Katnani HA, Van Opstal AJ, Gandhi NJ. A test of spatial temporal decoding mechanisms in the superior colliculus. *J Neurophysiol* 107: 2442–2452, 2012. First published January 25, 2012; doi:10.1152/jn.00992.2011.—Population coding is a ubiquitous principle in the nervous system for the proper control of motor behavior. A significant amount of research is dedicated to studying population activity in the superior colliculus (SC) to investigate the motor control of saccadic eye movements. Vector summation with saturation (VSS) has been proposed as a mechanism for how population activity in the SC can be decoded to generate saccades. Interestingly, the model produces different predictions when decoding two simultaneous populations at high vs. low levels of activity. We tested these predictions by generating two simultaneous populations in the SC with high or low levels of dual microstimulation. We also combined varying levels of stimulation with visually induced activity. We found that our results did not perfectly conform to the predictions of the VSS scheme and conclude that the simplest implementation of the model is incomplete. We propose that additional parameters to the model might account for the results of this investigation.

microstimulation; spatiotemporal; vector summation; vector averaging

WITH EXTERNAL ENVIRONMENTS rich in stimuli that continuously bombard our sensory systems, neural structures have the ability to store distributions of information that can be decoded by lower level structures to execute motor behavior. The saccadic system is well studied in this respect; specifically, research efforts have focused on motor control of saccadic eye movements to study ensemble activity in the superior colliculus (SC) (for a review, see Gandhi and Katnani 2011). In the visual domain, every potential target recruits a population of activity in the SC, and the distribution of information is somehow decoded to direct the line of sight to a desired object. As a result, studies have focused on target selection, revealing that reorientation toward a specific target can be probabilistic, depending on factors like saliency (McPeek and Keller 2002) and relative priority (Kim and Basso 2010; Mysore and Knudsen 2011). Once a population has been selected, however, the next crucial step is to transform the ensemble of collicular activity into a proper motor command for saccade generation. Insights into such decoding computations have been facilitated, in part, by the laminar layout of the SC and the topographical organization of saccade vectors. Recordings have indicated that the neural population of saccade-related cells in the motor map is well described by a Gaussian mound, in which neurons at the center fire maximally for the executed saccade vector, whereas cells away from the center exhibit lower firing rates (Ottes et al. 1986; Sparks et al. 1976). This investigation focuses specifically on how population firing patterns in the SC can be decoded to specify a saccadic command.

Different computational schemes have been proposed as potential mechanisms for decoding SC activity into a saccade vector: vector summation (VS) (Badler and Keller 2002; Brecht et al. 2004; Van Gisbergen et al. 1987), vector averaging (VA) (Brecht et al. 2004; Lee et al. 1988; Walton et al. 2005), and vector summation with saturation (VSS) (Goossens and Van Opstal 2006; Groh 2001). In all three models, the central premise is that each recruited cell, n, in the population contributes to the saccade by combining two factors: its activity, a_n (which could be the cell's mean or peak firing rate, or the number of spikes in the burst), and its fixed efferent connection strengths to the horizontal and vertical brain stem burst generators, $\vec{m}_n$, which are solely determined by the cell's location in the motor map. The SC population then determines the saccade vector, $\vec{S}$, by summing all weighted cell contributions:

$$\vec{S} = \gamma \cdot f\left[\sum_{n=1}^{N} a_n \cdot \vec{m}_n\right] \quad (1)$$

where N is the number of active cells, γ is a scaling factor, and $f[x]$ is the effective input-output characteristic of the brain stem. The three models differ in the way in which the scaling and the input-output function are implemented. In the VS and VA models, the latter is simply the identity ($f[x] = x$), whereas in the VSS model it is a sigmoid. In the VS and VSS models, the scaling parameter is a constant, whereas in the VA model it normalizes the total population activity (Lee et al. 1988)

$$\gamma = 1 / \sum_{n=1}^{N} a_n.$$

Vector averaging has garnered success by accounting for the findings from simultaneous suprathreshold microstimulation of two sites in the SC (Katnani and Gandhi 2011; Robinson 1972) and from local inactivation of the SC motor map (Lee et al. 1988). However, the VA scheme does not account for the observed relationship between the level of SC activity and saccade velocity (Berthoz et al. 1986; Goossens and Van Opstal 2000) or for the decrease in saccade amplitude with decreasing microstimulation strength (Groh 2011; Katnani and Gandhi 2010; Van Opstal et al. 1990). Moreover, it is not obvious how to implement the normalization factor physiologically (Groh 2001). In contrast, the VS model does not need an intricate nonlinear scaling mechanism to explain saccade decoding and readily accounts for the decrease of saccade amplitude with microstimulation strength. However, it cannot yield weighted vector averaging, which has been shown by

Address for reprint requests and other correspondence: H. Katnani, 203 Lothrop St., Eye & Ear Institute, Rm. 153, Univ. of Pittsburgh, Pittsburgh, PA 15213 (e-mail: hkatnani@gmail.com).

dual microstimulation experiments, nor does it generate fixed-vector saccades for suprathreshold microstimulation. By including output saturation, however, the VS model becomes the VSS scheme, which accounts for suprathreshold single and dual stimulation results, as well as for the results of local inactivation (Goossens and Van Opstal 2006; Groh 2001). So far, the VSS model has largely been tested for a single SC population. Because the environment typically provides multiple objects of interest, it is of importance to test the SC decoding mechanism with more challenging situations. The purpose of this investigation is to study the effects on saccades by inducing and manipulating two active populations in the SC with different stimulation strengths (Groh, 2001).

Figure 1 illustrates the hypothetical results of a VSS model tested with dual microstimulation. Figure 1*A* provides a temporal layout of a summation with saturation output for single (red and green) and dual microstimulation (blue) at different levels of activity. Figure 1*A* illustrates that when VSS is operating at high levels of activity, summation is constrained by saturation, and as result dual microstimulation resembles a weighted vector average. Figure 1*B* illustrates the spatial representation of a prediction that corresponds with outputs from dashed gray *box B*. Nevertheless, when VSS is operating at low levels of activity, summation is not constrained by saturation, and as a result dual microstimulation resembles vector summation. Figure 1*C* illustrates the spatial representation of a prediction that corresponds with outputs from dashed gray *box C*. Thus the model predicts a transition from resembling vector summation at low levels of activity to resembling vector averaging at high levels of activity (Groh 2001).

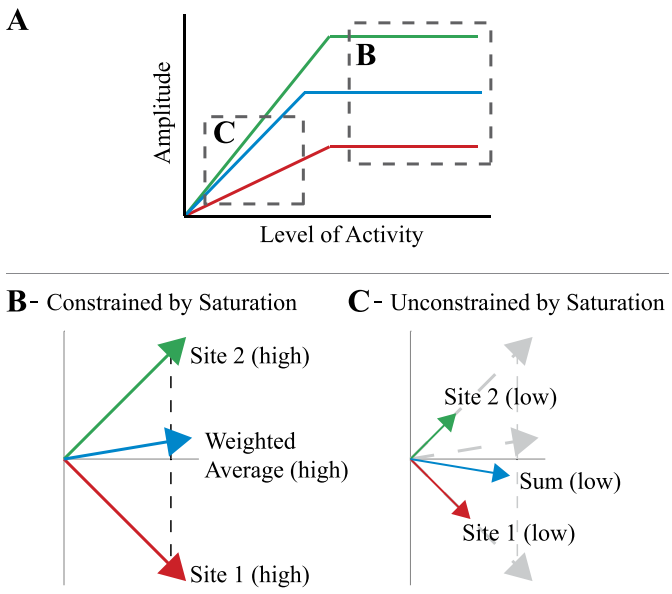

Fig. 1. Vector summation with saturation (VSS) predictions for stimulation-evoked vectors. *A*: temporal layout of the VSS predictions [adapted from Groh (2001)]. The red and green lines illustrate the result of stimulation at each individual site; the cyan line illustrates the output with dual microstimulation; and the dashed gray boxes illustrate the level of activity at which the model is operating to generate the predictions shown in *B* and *C*. *B* and *C*: spatial representation of a prediction that corresponds with outputs from dashed gray boxes in *A*. *Site 1* and *site 2* represent individual site-specific vectors evoked by high (*site 2*) or low (*site 1*) stimulation parameters and are shown as red and green lines, respectively. Simultaneous stimulation of the 2 sites produces the cyan vector [weighted average (high)/sum (low)]. Dashed black line in *B* represents all possible weighted average locations between the 2 site-specific vectors.

In contrast to the VSS predictions, we found that at both high and low stimulation strengths the movement elicited by dual-site microstimulation always resembled a weighted vector average of the movements evoked by the same level of activity at each site individually. This trend persisted even when low-level stimulation at one site co-occurred with activity for a visually evoked saccade at another site. Thus the output from two synchronous populations in the SC does not result from the independent summed contributions of the individual sites. Collectively, our results indicate that the VSS model, although appealing in its simplicity, does not explain the decoding of multiple active populations. We propose that extending the model with intracollicular interactions could account for the data observed in this study.

METHODS

All procedures were approved by the Institutional Animal Care and Use Committee at the University of Pittsburgh and complied with the guidelines of the Public Health Service "Policy on Humane Care and Use of Laboratory Animals."

Subjects and Surgical Procedures

Two juvenile male rhesus monkeys (*Macaca mulatta*) underwent one or more surgeries in a sterile environment and under isoflurane anesthesia. The initial procedure consisted of placing a Teflon-coated stainless steel wire (Baird Industries, Hohokus, NJ) under the conjunctiva of one eye and securing a head-restraint post to the skull. In the second procedure, one cylinder was cemented over a craniotomy. The chamber was placed stereotactically on the skull, slanted posteriorly at an angle of 38° in the sagittal plane. This approach allowed access to both colliculi and permitted electrode penetrations normal to the SC surface. After each surgery, the monkey was returned to its home cage and allowed to fully recover from surgery. Postoperatively, antibiotics and analgesics were administered as indicated in the protocol.

Experimental Procedures and Behavioral Tasks

Visual stimuli, behavioral control, and data acquisition were controlled by a custom-built program that uses LabVIEW architecture on a real-time operating system supported by National Instrument (Bryant and Gandhi 2005). Each animal was trained to sit in a primate chair with its head restrained, and a sipper tube was placed near the mouth for reward delivery. The animal sat inside a dome surrounded by two alternating magnetic fields that induced voltages in the eye coil and thus permitted measurement of horizontal and vertical eye position (Robinson 1963). The animal fixated targets that were projected onto a circular mirror, which rear reflects onto the isoluminant wall of the dome. Anti-warping software obtained from Paul Bourke, University of Western Australia, allowed reflections from the mirror to appear undistorted and for distances to be properly transferred onto a curved surface. The monkey sat in the center of the dome, which had a radius of 1 m and spanned ±150° horizontally and ±30° vertically of the visual field. A photodetector, positioned outside the animal's field of view, detected the actual time of appearance of visual objects, which was then used to correct for time shifts induced by the projector's refresh rate.

Both animals were trained to perform the oculomotor gap task. Every trial began with directing the line of sight to a fixation point for 300–500 ms before it was extinguished. After a 200- to 400-ms "gap" interval, during which the animal was required to maintain the same

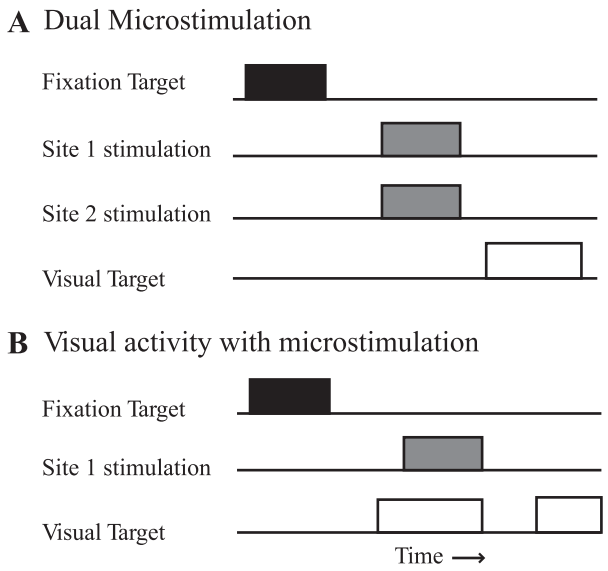

Fig. 2. Sequence of events for 2 experimental paradigms. *A*: timeline of events for dual microstimulation. *B*:timeline of events for visual activity with microstimulation. The onset, duration, and offset of each component in both paradigms is represented by blocked regions of different shades (black, fixation target; gray, site stimulation; white, peripheral target).

eye position, another stimulus was illuminated in a random location in the visual periphery. Incorporation of the gap interval permitted fixation to become disengaged before saccade preparation, allowing the oculomotor system to be more responsive to incoming visual and/or stimulation input (Sparks and Mays 1983). Each animal was permitted 500 ms to redirect its visual axis on the saccade target and hold gaze steady for 300–500 ms to earn a liquid reward. As the animal performed this task, two platinum iridium microelectrodes (1.0–1.5 MΩ; MicroProbes for Life Science, Gaithersburg, MD) were individually advanced with independent hydraulic microdrives (Narashige, Tokyo, Japan). The superficial layer of the SC was first identified by the presence of distinctive bursting of background activity associated with flashes of room lights. The electrode was then driven deeper into the SC until saccadic motor bursts were identified. At this stage, stimulation (40 μA, 400 Hz) was delivered during the gap interval to determine the vector coordinates. The depth of the electrode was then minimally adjusted to obtain the shortest possible latency of the stimulation evoked saccade (20–40 ms). Train duration was manually set (range: 100–300 ms) and was always long enough to allow for completion of the stimulation evoked movements.

Experiment 1: dual microstimulation. The objective of the first experiment was to assess the decoding mechanism based on saccades evoked by simultaneous stimulation of two SC sites. As illustrated in Fig. 2*A*, microstimulation was delivered 100 ms after fixation offset. After stimulation offset, a visual stimulus was presented in a random location in the periphery, to which the animal directed its visual axis to obtain a reward. Stimulation was delivered through either one electrode (10% of the trials per electrode) or through both electrodes (another 10% of trials). Initially, the stimulation parameters were suprathreshold (always set to 40 μA, 400 Hz, 100–300 ms, biphasic pulses). The current intensity and/or frequency through both electrodes were then reduced to a level that yielded nonoptimal saccades from each stimulation site. Table 1 lists the suboptimal parameters used for each paired site. Such saccades typically exhibit lower peak velocities and reduced amplitudes (Van Opstal et al. 1990), even with prolonged stimulation durations (Groh 2011; Guillaume and Pélisson 2001; Katnani and Gandhi 2010). The remaining 70% of control (nonstimulation) trials were pooled together to establish a database of visually guided saccades that were used for comparison with stimulation-evoked saccades.

Experiment 2: visually induced activity with microstimulation. Next, we examined the effect of microstimulation on visually guided

Table 1. *Suboptimal parameters used for each paired site*

Vector Pair	Site-specific Amplitude (*Site 1*/*Site 2*/Dual Site)	Lower Stimulation Setting (*Site 1*/*Site 2*)	Reduced Amplitude (*Site 1*/*Site 2*/Dual Site)
1	13.3/14.4/11.3	40 μA, 200 Hz/40 μA, 200 Hz	10.1/10.4/7.5
2	13.2/7/6.9	40 μA, 300 Hz/40 μA, 200 Hz	9/4.1/4
3	8.5/19.5/8.4	40 μA, 125 Hz/40 μA, 125 Hz	5.2/8.2/5
4	3.9/12.5/5.8	10 μA, 400 Hz/10 μA, 400 Hz	2.4/6.6/3
5	20/3.5/6.3	20 μA, 400 Hz/20 μA, 400 Hz	13.5/2.5/3
6	7.7/8.2/7.7	15 μA, 400 Hz/15 μA, 400 Hz	6.4/5.4/5.7
7	22.3/10.7/13.5	10 μA, 400 Hz/10 μA, 400 Hz	12.9/2.5/3.6
8	31.9/25.2/29.3	10 μA, 400 Hz/30 μA, 400 Hz	11.8/14.6/13.7
9	16.5/26.4/20.6	15 μA, 400 Hz/17 μA, 400 Hz	11.2/9.6/9.2
10	27.5/14.1/12.1	30 μA, 400 Hz/25 μA, 400 Hz	12.6/6.3/6.9
11	13.1/21.3/16.3	12 μA, 400 Hz/13 μA, 400 Hz	5.2/6/11.1
12	17.7/19/17.4	12 μA, 400 Hz/18 μA, 400 Hz	12.2/6.1/8.1
13	40.2/33.4/38.5	20 μA, 400 Hz/15 μA, 400 Hz	25.4/27/27.4
14	12.6/26/11.4	32 μA, 400 Hz/28 μA, 400 Hz	9.2/10.7/7.9
15	17.6/14.4/11.6	25 μA, 400 Hz/20 μA, 400 Hz	15.5/8.9/7.5
16	40/14.4/21.4	10 μA, 400 Hz/12 μA, 400 Hz	27.9/10/12.9
17	7.9/7.1/7.7	11 μA, 400 Hz/15 μA, 400 Hz	5.3/4.3/4.7
18	17.2/10.8/11.3	20 μA, 375 Hz/20 μA, 200 Hz	10.2/8.3/7.9
19	27/5.9/9.1	20 μA, 220 Hz/20 μA, 200 Hz	18/4.4/9
20	4.3/12.1/7.9	20 μA, 200 Hz/20 μA, 200 Hz	2.8/10.6/5
21	13.1/43/21.4	39 μA, 235 Hz/17 μA, 180 Hz	9.6/36.1/11.4
22	16.8/18.1/15.9	20 μA, 400 Hz/20 μA, 400 Hz	13.6/15.4/12.7
23	9.1/9.4/10.4	20 μA, 150 Hz/25 μA, 175 Hz	6.5/6.6/6.4
24	15.9/8.6/9.7	35 μA, 250 Hz/25 μA, 150 Hz	7.9/5.9/6.4
25	18.1/13/15.6	20 μA, 150 Hz/18 μA, 150 Hz	10.1/8.5/9.5
26	7.9/23.4/16.1	25 μA, 130 Hz/20 μA, 100 Hz	5.4/19.7/7
27	11.1/7.3/8.8	20 μA, 400 Hz/20 μA, 400 Hz	8.7/5.5/5.9
28	32.9/10.2/13.1	40 μA, 100 Hz/40 μA, 100 Hz	24.7/5.8/14.6
29	23.5/8.3/16.3	15 μA, 400 Hz/33 μA, 400 Hz	14.7/5.9/8
30	22.6/4.9/7.4	18 μA, 400 Hz/12 μA, 400 Hz	13.3/3.6/7.3

saccades. In 20% of gap saccade trials, microstimulation was delivered to one SC site during the presentation of a visual target (Fig. 2*B*), not during the gap period as in *experiment 1* described above. More specifically, the onset of the stimulation-evoked movement was timed to coincide with the typical saccade reaction time to the visual target. After a 200-ms blank period following stimulation offset, another visual target was presented in a random location in the visual periphery, which the monkey had to fixate to obtain a liquid reward. In another 10% of trials, however, stimulation was delivered to the electrode during the gap period (see Fig. 2*A*) to collect the saccade vector associated with the site and stimulation parameters.

The location of the visual target presented in relation to the evoked stimulation vector was loosely chosen to achieve distributions of distances in SC coordinates similar to those collected in *experiment 1*. Stimulation-evoked saccades that interacted with the visual target showed no obvious signs of curvature (saccades directed first toward one target and then toward the other in midflight; Arai et al. 2004; Port and Wurtz 2003) and reflected a weighted combination of the visual and stimulation-evoked saccades; only this subset of movements was analyzed for the purpose of this study. Saccades observed on other trials clearly resembled pure stimulation movements (stimulation onset occurred well before the visually guided saccade), curved saccades (stimulation onset occurred during the visually guided saccade), or pure visual movements (stimulation onset occurred after the visually guided saccade) (McPeek et al. 2003; Noto and Gnadt 2009) and were excluded from additional analyses. We note that movement of this nature were rarely observed during each session (<1% of data removed) because the stimulation onset spanned a narrow temporal range. As before, the experiment was first performed with suprathreshold stimulation parameters and then again repeated with stimulation settings that evoked reduced-amplitude saccades.

Electrical Stimulation

Constant-current stimulation trains were generated using a Grass S88X stimulator in combination with Grass PSIU6 isolation units. Trains consisted of anodal phase leading, biphasic pulses (0.25 ms). For high or suprathreshold stimulation conditions, current intensity and frequency were fixed at 40 μA and 400 Hz. The lower parameter space could be as low as 10 μA and 100 Hz, and differed for each data set to evoke reduced-amplitude saccades (see Table 1). Low stimulation settings were determined by selecting current intensities, frequencies, or both that reliably produced movements (>90% probability of evoking movement) but also significantly reduced the amplitude of the movements (~15% or more change in amplitude). Only one set of high- and low-stimulation-evoked saccades was collected for each data set, because the dual-stimulation protocol was only a small part of a larger stimulation study to systematically analyze the relationship between stimulation parameters and saccade features (Katnani and Gandhi 2010, 2011). In all cases, stimulation duration was always long enough to ensure that it outlasted the eye movement.

Data Analyses

Each trial was digitized and stored for off-line analysis. We used a combination of in-house software and Matlab 7.10.0 (R2010a). Horizontal and vertical eye position along with onset and offset times of the stimulation train were stored with a resolution of 1 ms. Component velocities were obtained by differentiating the eye position signal. Onset and offset of stimulation-evoked saccades were then detected using a standard 30°/s velocity criterion, respectively.

Eye movements evoked during simultaneous stimulation or during stimulation with visual stimuli were quantified using two techniques. The first analysis uses a straightforward Euclidean metric. We compared the predictions of the VSS computation to actual data by simply calculating the magnitude of each elicited vector and the magnitude of the respective vector addition prediction.

The second analysis used a multilinear regression:

$$V_3 = A \cdot V_1 + B \cdot V_2. \quad (2)$$

The analysis was performed for each vector pair elicited by high and low stimulation settings. The two coefficients A and B define the single-site vector (V_1 and V_2) contribution to the output (V_3). The sum of the coefficients describes where the vector falls in relation to the single-site vectors. For example, coefficients that sum to 1 identify a weighted vector averaging response, whereas a sum of 2 indicates vector summation. Two pieces of information are noteworthy about the regression technique. First, a coefficient sum of 1 does not imply that each site contributes half its vector (coefficients equaling 0.5) because averaging movements can be rotated due to the weight/contribution from each site being different. Second, during simultaneous stimulation, we do not know how the single-site vectors interact to contribute to the elicited averaging movements. Therefore, we must assume that these independent vectors are conveyed by the single-site stimulation trials collected under each parameter setting. To ensure that each of the individual vectors was well characterized, we bootstrapped the single-site endpoint distributions, with replacement, and averaged across them.

RESULTS

Analysis of Microstimulation-Elicited Saccade Features

Here we provide a robust characterization of saccades evoked by low stimulation parameters. We demonstrate that using low vs. high stimulation parameters produces significant and reliable changes in saccade properties that help to assess whether such movements can be accommodated for by decoding models.

We report on a total of 30 stimulation-induced saccade-vector pairs obtained from two monkeys, sampling a range of the SC motor map that spanned ~2° to 45° in amplitude and approximately −80° to 80° in direction (Fig. 3). The vector pairs exhibited radial amplitude differences between 0° and 28° and directional differences between 20° and 100°. To reduce the amplitude of saccade vectors, current intensity (18 sites), frequency (4 sites), or both (8 sites) were lowered at each electrode. We found that regardless of the stimulation

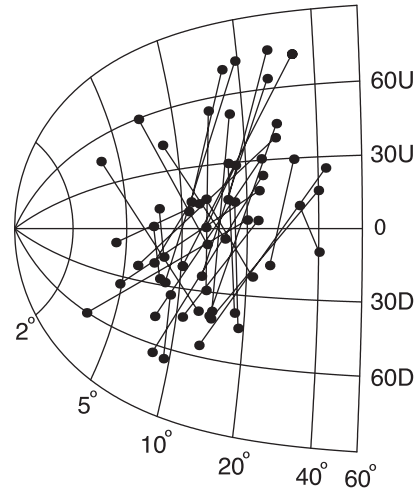

Fig. 3. Distribution of paired stimulation sites. The vector evoked by each site is shown by a black dot, and the pair is connected by a line. All 30 paired sites are represented on the superior colliculus (SC) saccade motor map. Numbers spanning from *left* to *right* indicate saccade amplitude. Vertically aligned text (*right*) denotes saccade direction: U, up; D, down.

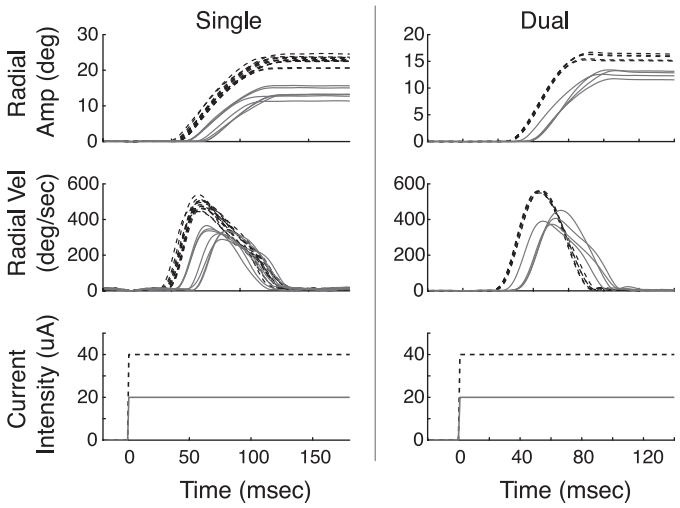

Fig. 4. Traces of stimulation-evoked saccades. *Left*: radial amplitude (*top*) and radial velocity (*middle*) for saccades evoked by high (black dashed traces) and low (solid gray traces) stimulation parameters for a single site in the SC. *Bottom* row illustrates the different current intensity used to generate each distribution of traces. *Right*: same conventions as at *left*, but for saccades generated by simultaneous stimulation of 2 sites in the SC.

parameter lowered, we could reliably produce a smaller-than-optimal saccade vector for single or dual stimulation sites in the SC (see Table 1). Furthermore, the saccade always completed within the train duration. Figure 4 illustrates the radial amplitude and radial velocity of saccades produced by high (40 μA) and low (20 μA) current intensities from single (*left*) and dual (*right*) stimulation sites. Figure 4 provides insight into the differences generated in saccade features when stimulating at high and low levels. One can observe a reduction in amplitude, a significant shift in response latency, and more variability in the amplitude and velocity traces.

To characterize these differences across all stimulation-evoked saccade vectors (single and dual stimulation sites), we categorized each data set into a high or low group based on the stimulation parameters that evoked them. Figure 5*A* illustrates the radial amplitude of saccades in the high vs. low groups (*site 1*, red; *site 2*, green, dual site, cyan) using a log-log plot. Almost all points are below the line of unity, demonstrating a significant reduction in amplitude (paired *t*-test, $P < 0.001$). To assess variability, vector distributions of radial amplitude and peak velocity were normalized by their respective mean values obtained from the same site and with the same stimulation parameters. The normalized distributions across all data sets were then pooled together, and the high and low groups were compared. Figure 5, *B* and *C*, illustrates the normalized distributions pooled across all sites of radial amplitude and peak velocity, respectively, generated by high stimulation parameters compared with those generated by low stimulation parameters; notice the larger variability introduced by lower stimulation parameters. Observing that the data distribution is nearly Gaussian, we performed *F*-tests to assess whether dual-site stimulation at high or low levels produced less variability in the different saccade distributions than those generated by single-site stimulation. We found no significant differences in the distributions produced by high-level stimulation. Distributions for low-level stimulation were always more variable than those produced by high-level stimulation. Interestingly, however, dual-site stimulation at low levels generated significantly less variability in radial amplitude and radial velocity compared with single-site stimulation (radial amplitude: *F*-test, $P < 0.05$; radial velocity: *F*-test, $P < 0.05$).

To characterize the kinematics of saccades produced by low stimulation parameters, we have illustrated the main sequence properties (Fig. 6, *A* and *B*) and the skewness of the velocity profiles compared with those of visually guided saccades. Figure 6, *A* and *B*, demonstrates that lower stimulation parameters generate slower and longer duration saccades, even when elicited by dual-site stimulation (*site 1*, red triangles; *site 2*, green squares; dual site, cyan circles). All peak velocity and duration distributions generated by low stimulation parameters (single and dual site) were significantly different from visually guided distributions [peak velocity: Kolmogorov-Smirnoff (KS) test, $P < 0.001$; duration: KS test, $P < 0.001$]; furthermore, distributions generated by dual-site stimulation were not significantly different from those generated by single-site stimulation (peak velocity: KS test, $P > 0.11$; duration: KS test, $P > 0.34$). Neither the peak velocity nor duration of saccades produced by high stimulation parameters was significantly different from that of visually guided saccades (KS test, $P > 0.4$; data not shown).

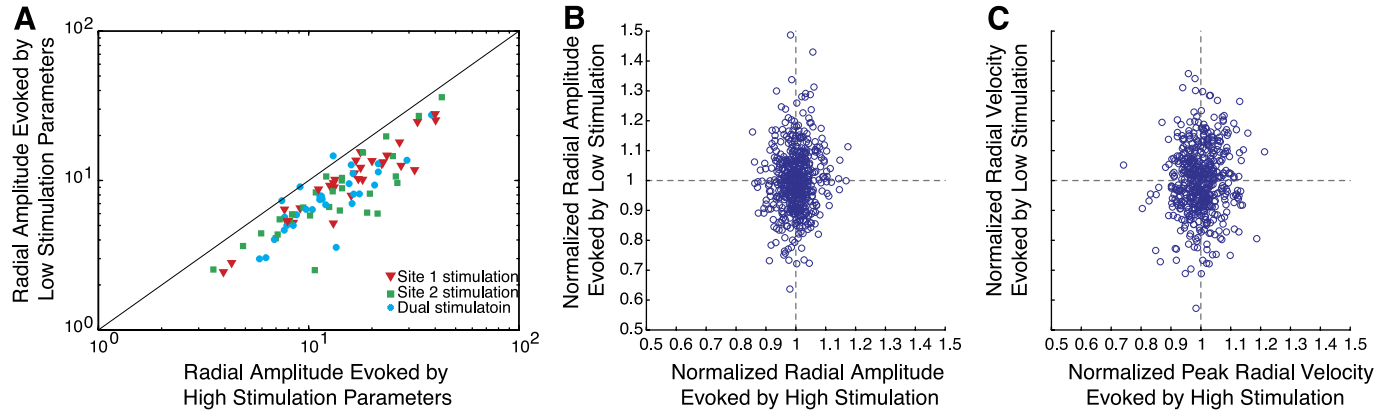

Fig. 5. Saccade features of stimulation-evoked movements. *A*: correspondence of mean radial amplitude between saccades evoked by high vs. low stimulation parameters. Filled red triangles and green squares represent the mean radial amplitude of saccades evoked by single-site stimulation (*site 1* and *site 2*); cyan dots represent the mean radial amplitude of saccades evoked by dual-site stimulation. *B*: normalized radial amplitudes evoked by high vs. low stimulation parameters. *C*: normalized radial velocities evoked by high vs. low stimulation parameters. Note the larger spread of data points along the *y*-axis in *B* and *C* demonstrates that saccade features evoked by low stimulation parameters have greater variability.

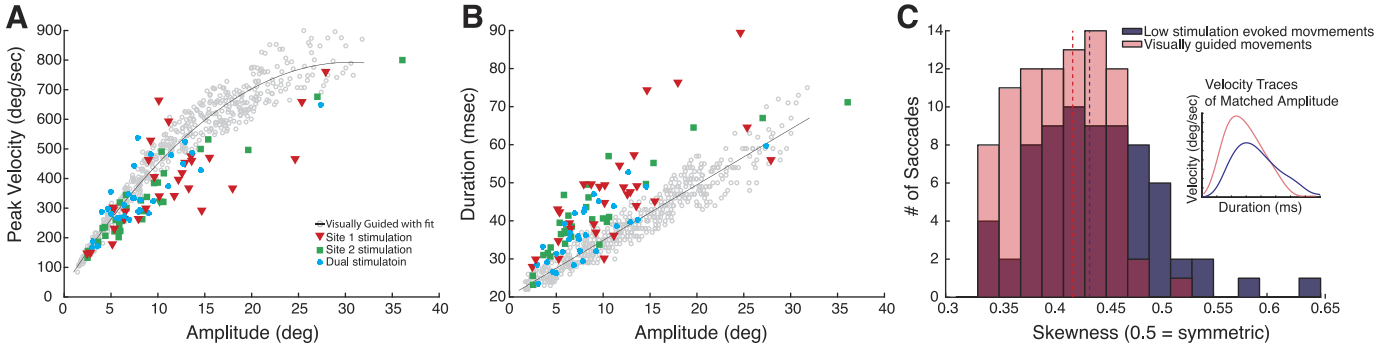

Fig. 6. Kinematics of saccades produced by low stimulation parameters. Mean radial amplitude vs. mean peak velocity (*A*) and mean duration (*B*). Filled red triangles and green squares represent main sequence properties for saccades evoked by low stimulation parameters at a single site; cyan dots represent properties for saccades evoked by dual-site stimulation. Gray circles and solid black line represent sequence properties and fit for visually guided saccades, respectively. *C*: histogram comparison of the skewness values calculated for visually evoked (transparent red) and stimulation-evoked movements (blue) that fall within an amplitude bin that ranges from 2° to 16°; dashed lines indicated the median for the color-matched distribution. *Inset*: example velocity trace for visually guided (transparent red) and stimulation-evoked movements (blue) of similar amplitude (~19°).

As can be seen in Fig. 6, *A* and *B*, the majority of stimulation points fall within an amplitude bin that ranges from 2° to 16°. We calculated and compared the skewness of all stimulation-evoked and visually evoked saccades within this range (Fig. 6*C*). The velocity profiles generated from low stimulation conveyed the typical positive skewness (time to peak velocity divided by total saccade duration is usually <0.5; Van Opstal and Van Gisbergen 1987) seen in visually guided saccades. However, the *inset* of Fig. 6*C* provides an example of how low stimulation parameters tend to generate broader peaks as a result of lower peak velocities and longer durations. Figure 6*C* summarizes the result by comparing the distributions of skewness for eye movements evoked by low stimulation (blue) and those generated by visual stimuli (red). Note that values equal to 0.5 signify symmetry, those greater than 0.5 signify positive skewness, and those less than 0.5 signify negative skewness. The median of blue distribution (0.44; blue dashed line) was significantly different (rank sum, $P < 0.01$) from that of red distribution (0.41; red dashed line), indicating more symmetric velocity profiles.

Simultaneous Dual Microstimulation

Having shown that lower stimulation parameters reliably reduce the radial amplitude of evoked saccades, we can now utilize different levels of microstimulation as a tool to explicitly test the predictions of collicular decoding schemes. Figure 7*A* illustrates results of high and low stimulation for one vector pair. Open symbols represent high or suprathreshold stimulation endpoints (40 μA, 400 Hz). The dashed red and green traces denote the spatial trajectories elicited at each site in the vector pair; the dashed cyan lines are the result of dual-site stimulation with the same suprathreshold parameters. The dashed black line connecting the single-site endpoint distributions represents all possible weighted average locations between the two vectors. Note that the dual-stimulation endpoints lie close to the vector average line. When the experiment was repeated with lower stimulation parameters at each electrode (40 μA, 200 Hz), the endpoints generated by single-site stimulation, as well as by dual stimulation, scaled back together (filled endpoints). The solid black line, connecting the single-

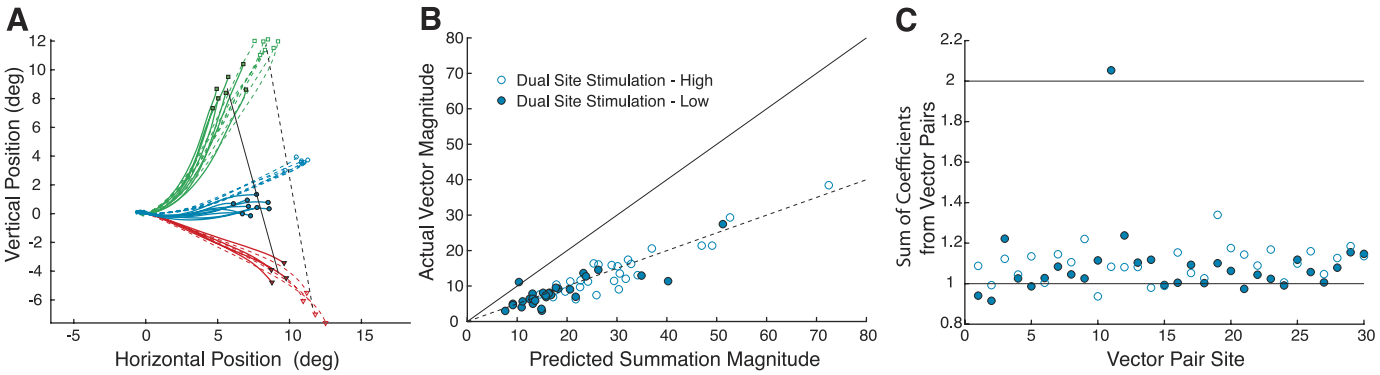

Fig. 7. Simultaneous dual microstimulation results. *A*: dashed red and green trajectories represent the individual site-specific vectors elicited by high stimulation parameters (40 μA, 400 Hz) and are shown with their corresponding endpoint distributions, open red triangles and open green squares. Simultaneous stimulation of the 2 sites produced the dashed cyan trajectories with cyan circle endpoints. Solid red and green trajectories represent the reduced-amplitude vectors elicited at each individual site by low stimulation parameters (40 μA, 200 Hz) and are shown with their corresponding endpoint distributions, filled red triangles and filled green squares. Simultaneous stimulation of the 2 sites with low stimulation parameters produced the solid cyan trajectories with cyan dot endpoints. The dashed line between the 2 site-specific vectors and the solid line between the 2 individual reduced-amplitude vectors represent all possible weighted average locations. *B*: comparison of mean radial amplitudes elicited by dual-site stimulation vs. the summed amplitude of paired site-specific movements. Solid black line represents perfect correspondence between predicted summation and actual response; dashed black line represents perfect correspondence between predicted averaging and actual response. *C*: collected vector pairs vs. sum of multilinear regression coefficients. Solid line at 1 indicates averaging responses; solid line at 2 indicates summation responses. In *B* and *C*, open cyan circles represent mean amplitude or coefficient sums evoked by high stimulation parameters, and filled cyan circles represent mean amplitude or coefficient sums evoked by low stimulation parameters.

site endpoints, represents all weighted average locations between the two reduced-amplitude vectors. Thus Fig. 7*A* shows that at both high and low stimulation settings, dual-site stimulation produced movements that resembled a weighted vector average.

To summarize the results for all vector pairs ($n = 30$ paired sites), we plotted (Fig. 7*B*) the magnitude of the sum of paired site-specific movements, at both high (open circles) and low (filled circles) stimulation, versus the actual magnitude of the movement elicited by dual-site stimulation. Figure 7*B* illustrates that the majority of points fall below the unity line and lie close to the half-slope of the line (dashed line), confirming an absence of linear addition and showing a dominant averaging response. The consistency of the results across all high and low stimulation parameters highlights the insensitivity of the mechanism to the chosen stimulation settings. We also performed multilinear regression, in which the sum of coefficients derived from the regression of each vector pair (see METHODS) quantifies where movements elicited by dual stimulation fall within the spectrum of averaging (sum of coefficients equals 1) to linear summation (sum equals 2). Figure 7*C* illustrates that the summed parameters values for almost all low (filled circles; mean 1.09, SD 0.19) and high stimulation strengths (open circles; mean 1.09, SD 0.08) were about 10% larger than 1. The parameter distributions generated by high and low stimulation strengths were not significantly different from one another (*t*-test, $P = 0.91$).

In an attempt to observe any trends that could provide insight into the dominant averaging response, the sum of coefficients generated from each vector pair was correlated to spatial and temporal saccade features (i.e., directional separation between saccade vectors, location on the SC motor map, radial amplitude differences, and latency differences). Because of the minimal variability generated in the distribution of coefficient sums, the analysis revealed no trends. Notice, however, that a single vector pair did exhibited vector summation (coefficient sum = 2.05). Unfortunately, the saccade features for the data set did not differ from all other vector pairs that conveyed averaging responses.

Interactions of Visually Guided and Stimulation-Evoked Saccades

When testing the VSS model with dual microstimulation, we observed that the evoked saccades did not meet the linear predictions of the model. Furthermore, we found that the kinematics of movements elicited by lower stimulation parameters did not match those generated by visually guided saccades. Since it is unclear how microstimulation induced activity to generate such saccades, it might be argued that the observed averaging outcome is a result of an inadequate drive provided by dual microstimulation. Therefore, we replaced one of the two loci with visual target-driven activity to observe whether any changes occur when part of the total SC population is generated by natural activation.

We studied a total of 22 vector pairs, sampling a portion of the SC saccade vector map that spanned ~7° to 36° in amplitude and approximately −90° to 70° in direction (Fig. 8; gray dots, visual targets; black dots, stimulation sites). The visually guided movements and stimulation-induced movements exhibited radial amplitude differences anywhere between 0° and 21° and directional differences between 22° and 123°. We found that stimulation onset coinciding just before the onset of the saccade to the visual target generated a straight trajectory whose amplitude and direction were influenced by both the visual target and the stimulation-evoked movement. (Note: for simplicity we will call these movements VE saccades). Accordingly, the addition of the mean stimulation site latency (high parameter setting: 29 ms, SD 9 ms; low parameter setting: 90 ms, SD 30 ms) to the onset of stimulation relative to the presentation of the visual target (high parameter setting: 171 ms, SD 27 ms; low parameter setting: 116 ms, SD 45 ms) approximately equaled the mean reaction time of the visually guided saccades (212 ms, SD 33 ms).

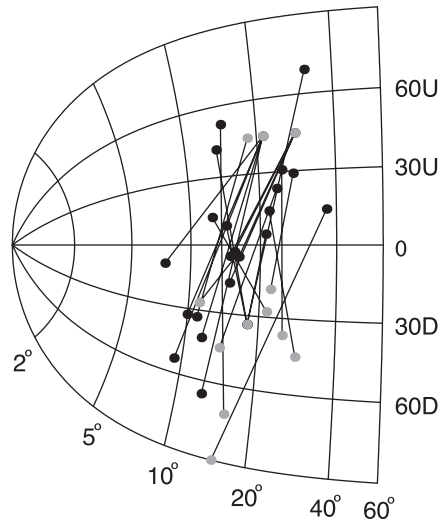

Fig. 8. Distribution of paired visual and stimulation sites. Each vector evoked by stimulation is shown by a black dot; each vector evoked by the presentation of visual target is shown by a gray dot. The pair is connected by a line. All 22 paired sites are represented on the SC saccade motor map. Numbers spanning from *left* to *right* indicate saccade amplitude. Vertically aligned text (*right*) denotes saccade direction.

We reduced the evoked amplitudes for single stimulation sites by varying current intensity (12 sites), frequency (2 sites), or both (8 sites). Figure 9*A* illustrates VE saccades (cyan trajectories) produced at both high (40 μA, 400 Hz; open circles) and low stimulation parameters (15 μA, 400 Hz; filled circles) for a single vector pair. The red trajectories correspond to the single-site stimulation at high (open triangles) and low parameter settings (filled triangles), whereas the green trajectories represent saccades made to the visual target. As with the dual-site stimulation results, the endpoints of the VE saccades, evoked by either high or low stimulation parameters, more closely resembled weighted vector averaging responses than linear vector summation, although responses were systematically larger than the weighted average for both stimulation strengths. Figure 9*B* illustrates a summary of the results across all vector pairs by comparing the magnitude of the summation prediction with the magnitude of the movement elicited by stimulation. Regardless of the stimulation settings, high (open circles) or low (filled circles), nearly all points fall below the solid unity line and close to the half-slope of the line (dashed line). In addition, multilinear regression (Fig. 9*C*) revealed that almost all low (filled circles; mean 1.13, SD 0.27) and high stimulation values (open circles; mean 1.16, SD 0.12) were about 14% larger than 1. The distributions were not signifi-

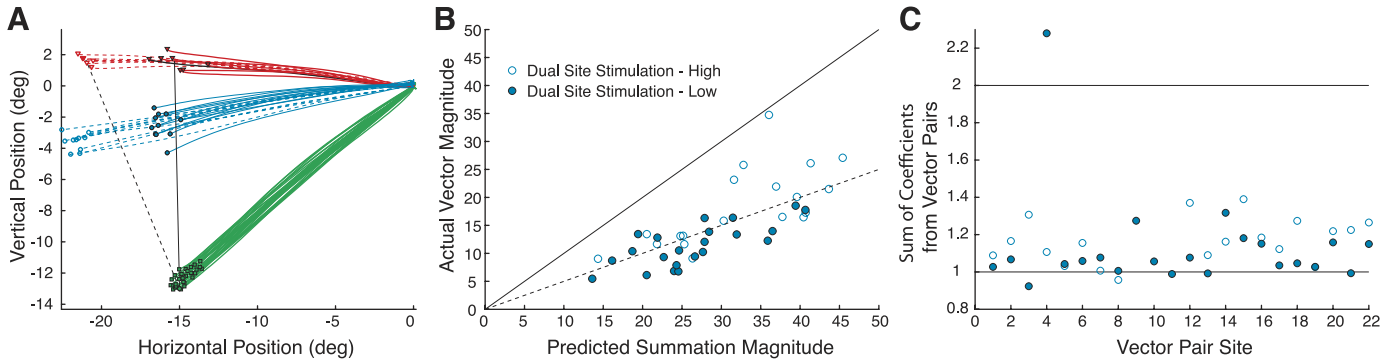

Fig. 9. Visually induced activity with microstimulation results. *A*: dashed red lines and open red triangles represent the trajectories and endpoints elicited by high stimulation parameters (40 μA, 400 Hz); solid green lines and squares represent trajectories and endpoints made to the presented visual target; dashed cyan lines and open cyan circles represent trajectories and endpoints of VE saccades evoked with visual activity and high stimulation parameters. Solid red lines and triangles represent trajectories and endpoints elicited by low stimulation parameters (15 μA, 200 Hz); solid cyan lines and dots represent trajectories and endpoints of VE saccades evoked with visual activity and low stimulation parameters. The dashed line between the site-specific vectors and visual target and the solid line between the reduced-amplitude vector and visual target represent all possible weighted average locations. *B*: comparison of mean radial amplitudes for VE saccades vs. the summed amplitude of paired site-specific movements. Solid black line represents perfect correspondence between predicted summation and actual response; dashed black line represents perfect correspondence between predicted averaging and actual response. *C*: collected vector pairs vs. sum of multilinear regression coefficients. Solid line at 1 indicates averaging responses; solid line at 2 indicates summation responses. In *B* and *C*, open cyan circles represents mean amplitude or coefficient sums evoked by visual activity with high stimulation parameters, and filled cyan circles represents mean amplitude or coefficient sums evoked by visual activity with low stimulation parameters.

cantly different from one another (*t*-test, $P = 0.63$). We note that, again, one vector pair exhibited summation-like results (coefficient sum = 2.27) with no distinct differences to provide insight to the outlying result. Furthermore, we compared the saccade features of the vector pair with a dual-site microstimulation pair that also conveyed summation. No similarities were found, because the two pairs were different in amplitudes, directions, amount of amplitude reduction, and vector separation.

The main sequences of VE saccades (Fig. 10; red triangles) were not significantly different (KS test, $P = 0.869$) from those evoked by simultaneous stimulation of two sites with low stimulation parameters (cyan dots). The peak velocities and durations of VE saccades were significantly smaller and longer than those of visually guided movements (Fig. 10, black traces; peak velocity: KS test, $P < 0.001$; duration: KS test, $P < 0.001$). Furthermore, the skewness of VE saccades was also similar to the dual stimulation results, exhibiting broader peaks as a result of lower peak velocities and longer durations (data not shown).

DISCUSSION

VSS makes an experimentally testable prediction for low vs. high levels of activity at two simultaneous populations in the SC motor map. Specifically, the model predicts that the low-level activities generate a vector that resembles the linear addition of the two single-site vectors, whereas the result of high activity at each site resembles the weighted vector average of the two single-site saccades (Fig. 1) (Groh 2001). We found that at both high and low stimulation levels, the evoked movements always resembled a weighted vector average of the two individual saccade vectors (Fig. 7). As a result, we conclude that the VSS decoding scheme in its simplest form is insufficient to properly describe spatiotemporal decoding of multiple populations of activity in the oculomotor system.

Interpreting Microstimulation

Microstimulation is arguably a crude technique that requires further study to understand how stimulation parameters (i.e., current intensity and frequency, neural circuitry) relate to evoked behavior (Katnani and Gandhi 2010). Yet, stimulation studies using suprathreshold parameters have yielded saccades with metrics that closely matched the movement fields of nearby cells recorded with the same electrode and kinematics that were indistinguishable from visually guided saccades of the same amplitude. At lower current intensities (Van Opstal et al. 1990) or frequencies (Stanford et al. 1996), evoked saccades have smaller amplitudes and velocities that fall below the

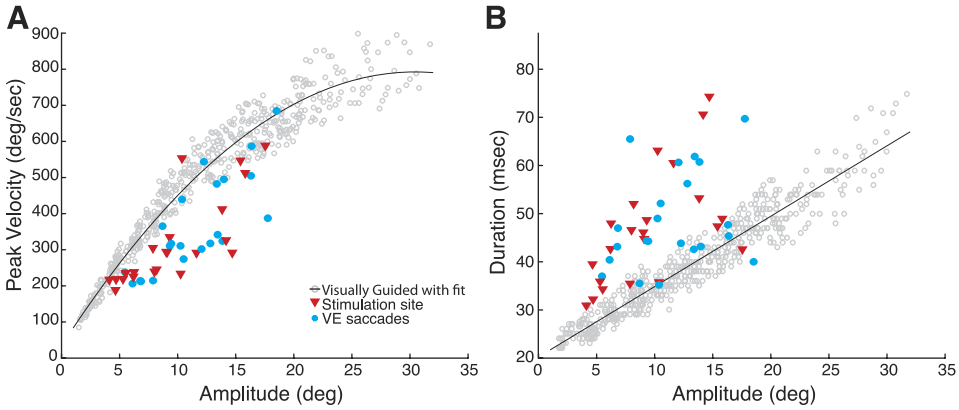

Fig. 10. Kinematics of stimulation-evoked saccades and VE saccades. Mean radial amplitude vs. mean peak velocity (*A*) and mean duration (*B*). Filled red triangles represent main sequence properties for saccades evoked by low stimulation parameters at a single site; filled cyan circles represent properties for VE saccades. Solid black line in *A* and *B* represents a fit of the main sequence properties for visually guided saccades (gray circles).

normal main sequence. These findings can in principle be explained by different mechanisms. For example, microstimulation might induce an electric field around the electrode tip that results in a Gaussian activation pattern, the size and height of which depend on the stimulation parameters. Suprathreshold microstimulation then produces neural activity that resembles the activity for normal visually guided saccades. Lowering current intensity reduces the passive spread of the electric field (Ranck 1975; Stoney et al. 1968), whereas lowering the pulse-train frequency reduces the local strength of the electric field (Ranck 1975; Tehovnik 1996). Both manipulations decrease the total input strength to the cells, leading to a smaller population response and thus slower and smaller saccades. An alternative explanation could be that only a few cells near the electrode tip are directly activated by the electric field (Histed et al. 2009) and that the total population response results from synaptic transmission through the local intracollicular network (McIlwain 1982). The effectiveness of this transmission could then systematically depend on both the current intensity and frequency (stimulation strength).

Either assumption can explain the dependencies of the population (and resulting saccade) output on microstimulation parameters. Importantly, the high similarities between electrically and visually elicited movements strongly suggest that SC population responses are decoded in the same manner, regardless of their cause. Thus we can utilize microstimulation to manipulate the stereotypical responses generated by the oculomotor system to gain more insight into spatiotemporal decoding mechanisms.

Interpreting an Absence of Linear Addition

Contrary to the prediction of the VSS model, we did not observe linear addition when simultaneously stimulating two sites in the SC with low stimulation parameters. Here we discuss whether such a result is evidence against a summation mechanism or is due to the methodology. We consider two potential issues that could mask linear addition.

First, reduced-amplitude saccades evoked by single- and dual-site stimulation could be the result of truncation due to insufficient pulse-train duration (Van Opstal et al. 1990). Stanford et al. (1996) demonstrated that when using low-frequency pulse trains, stimulation duration has to be increased to yield the same saccade. However, closer examination of their results suggests that low stimulation frequencies could produce changes in saccade amplitude at all applied train durations. A recent study by Groh (2011) also demonstrated a reduction in saccade amplitude at lower stimulation frequencies (and initial eye-in-head position). Our data are in agreement with this finding, because smaller amplitude saccades evoked by low current and/or frequency were always completed well before the stimulation offset. Therefore, we consider it unlikely that a lack of linear addition would result from insufficient train duration.

Second, could averaging be an artifact of dual microstimulation? Low current intensity and/or frequency might induce population profiles that result in weak excitation. Previous research suggested a balance between local excitation and global inhibition during the execution of normometric saccades (Hikosaka and Wurtz 1985a, 1985b). Therefore, total motor activity induced by low stimulation parameters may drive the balance between excitation and inhibition in an inadequate fashion; this could potentially mask the true intent of decoding. To account for this possibility, we performed an additional experiment in which one of the two stimulation sites was replaced with a visual target. The introduction of visually induced activity would allow the preparation of a normal motor command that should correspond to the natural excitation-inhibition dynamics of the system. We reasoned that the visually guided movement would always drive the system close to saturation, and therefore the combination of the movement with either high or low stimulation parameters should evoke saccade amplitudes constrained by saturation. Contrary to this prediction, low-level stimulation evoked responses with smaller amplitudes than the visual saccades as a result of being the weighted average between the visual target and the reduced stimulation vector (see Fig. 9). Furthermore, the velocity profiles of the evoked movements exhibited lower peak velocities and longer durations, similar to saccades evoked by dual-site microstimulation. Therefore, it is unlikely that the observed averaging result is an artifact of dual microstimulation.

Decoding Mechanisms

Three decoding mechanisms have been proposed in the literature to explain spatiotemporal decoding in the oculomotor system: vector averaging (VA), vector summation (VS), and vector summation with saturation (VSS). Here we discuss how each mechanism relates to the data obtained in *experiments 1* and *2*.

As explained in the Introduction, the VA scheme in its strictest sense depends only on the stimulation site and therefore does not produce smaller saccade amplitudes and has no mechanism to influence saccade kinematics. Although the outcome of our data exhibits vector averaging (Figs. 7*B* and 9*B*), the VA model would not predict a difference in amplitude, or kinematics, when changing from high to low levels of stimulation. To account for these findings, two mechanisms have been added to the VA model: *1*) firing rates in the brain stem burst generator covary with SC activity levels (Nichols and Sparks 1996; Sparks and Mays 1990), and *2*) a change in the normalization factor (*Eq. 1*) to

$$\gamma = 1 / \left(K + \sum_{n=1}^{N} a_n \right)$$

allows the averaging scheme to yield reduced-amplitude saccades (Van Gisbergen et al. 1987; Van Opstal and Goossens 2008). In this way, the vigor of activity in the SC influences the gain of the brain stem burst generator, and the addition of K as a constant in the normalization (in spikes/s) can influence the amplitude of decoded saccades. For example, if the total population activity in the SC is low, K can dominate the denominator to reduce the amplitude of the saccade. The scheme then resembles the vector summation model (see *Eq. 1*, where $\gamma = 1/K$). If the population activity is high, K becomes negligible and the computation approaches vector averaging. However, by extending the VA computation in such a manner, the model becomes a VSS scheme (generating the same predictions) in which saturation is implemented at high levels of activity through normalization (equivalent to reaching a threshold level).

A recent proposal of vector summation (Goossens and Van Opstal 2006) states that the saccade goal is computed by the summation of mini-vectors elicited by each spike of active cells in a population. The SC motor map thus specifies the desired saccade trajectory, including its kinematics. As a result, saccade vectors now depend strongly on activity level. This allows the model to predict differences in saccade metrics and kinematics when tested with high vs. low activity for one motor command. However, the VS model assumes that SC cells are independent units and that weighting occurs entirely downstream of the motor map; therefore, the model cannot account for multiple population decoding (i.e., *experiments 1* and *2*) and needs an additional criterion to constrain eye movements.

VSS establishes a decoding mechanism that can define how much of the total activity from the SC motor map actually contributes to a movement. However, neurons in the SC are still assumed to be independent units, and the summation of their spikes is only constraining once a threshold is reached (Goossens and Van Opstal 2006; Groh 2001). As a result, the model predicts linear addition at low levels of activity when the threshold is not met, but this prediction was not confirmed by our data. To account for the findings in this investigation, we speculate that excitatory and inhibitory interactions in the motor map are critical for limiting a summation mechanism. Evidence suggests that lateral interactions are involved in shaping stimulation-induced activity (see *Interpreting microstimulation* above); therefore, the addition of intracollicular interactions (Lee and Hall 2006; Meredith and Ramoa 1998; Munoz and Istvan 1998; Pettit et al. 1999) would allow the model to account for the possibility that multiple sites within the SC motor map compete through lateral inhibitory connections. Under these circumstances, both sites would have reduced firing rates (and hence lead to slower saccades), resulting in a reduction of the total number of spikes. Therefore, the interactions provide a method in which the summation of spikes could be constrained at both high and low activity levels. Further evidence is needed to corroborate interactions as a constraining mechanism. Nevertheless, naturally evoked saccades have been shown to land in intermediate location relative to multiple visual stimuli ("global effect") (Coren and Hoenig 1972; Godijn and Theeuwes 2002). An experiment that utilizes two-site recording in the SC to correlate naturally induced neural activity to global effect behavior could potential validate the interaction mechanism. Previous experimentation in the SC (Edelman and Keller 1998; McPeek et al. 2003; Port and Wurtz 2003; Van Opstal and Van Gisbergen 1990) would provide a foundation for the significance of such work.

Finally, we speculate that intracollicular interactions need not be the definitive mechanism to constrain summation. For example, interactions between concurrent motor commands can occur at other nodes of the oculomotor neuraxis (e.g., frontal eye fields, basal ganglia). Also, the gating of the saccadic system by the pontine omnipause neurons (OPNs) is a function of saccadic velocity (Yoshida et al. 1999). Since eye velocity is attenuated for low-frequency stimulation, the OPNs may resume earlier, thus limiting the magnitude of the stimulation-evoked movement. Additional studies are required to probe the potential contributions of these mechanisms.

ACKNOWLEDGMENTS

We thank J. McFerron for programming maintenance and G. Foster for general assistance.

GRANTS

H. A. Katnani is supported by National Institutes of Health (NIH) Grant T32 GM081760 and National Science Foundation Grant DGE-0549352. N. J. Gandhi is supported by NIH Grants R01 EY015485, P30 EY008098, and P30 DC0025205. A. J. Van Opstal is supported by the Radboud University Nijmegen and a VIDI Netherlands Organization for Life Sciences Research (NWO/ALW) Grant 805.05.003.

DISCLOSURES

No conflicts of interest, financial or otherwise, are declared by the author(s).

AUTHOR CONTRIBUTIONS

Author contributions: H.A.K., A.J.v.O., and N.J.G. conception and design of research; H.A.K. performed experiments; H.A.K. analyzed data; H.A.K., A.J.v.O., and N.J.G. interpreted results of experiments; H.A.K. prepared figures; H.A.K. drafted manuscript; H.A.K., A.J.v.O., and N.J.G. edited and revised manuscript; H.A.K. approved final version of manuscript.

REFERENCES

Arai K, McPeek RM, Keller EL. Properties of saccadic responses in monkey when multiple competing visual stimuli are present. *J Neurophysiol* 91: 890–900, 2004.

Badler JB, Keller EL. Decoding of a motor command vector from distributed activity in superior colliculus. *Biol Cybern* 86: 179–189, 2002.

Berthoz A, AG JD. Some collicular efferent neurons code saccadic eye velocity. *Neurosci Lett* 72: 289–294, 1986.

Brecht M, Singer W, Engel AK. Amplitude and direction of saccadic eye movements depend on the synchronicity of collicular population activity. *J Neurophysiol* 92: 424–432, 2004.

Bryant CL, Gandhi NJ. Real-time data acquisition and control system for the measurement of motor and neural data. *J Neurosci Methods* 142: 193–200, 2005.

Coren S, Hoenig P. Effect of non-target stimuli upon length of voluntary saccades. *Percept Mot Skills* 34: 499–508, 1972.

Edelman JA, Keller EL. Dependence on target configuration of express saccade-related activity in the primate superior colliculus. *J Neurophysiol* 80: 1407–1426, 1998.

Gandhi NJ, Katnani HA. Motor functions of the superior colliculus. *Annu Rev Neurosci* 34: 203–229, 2011.

Godijn R, Theeuwes J. Programming of endogenous and exogenous saccades: evidence for a competitive integration model. *J Exp Psychol Hum Percept Perform* 28: 1039–1054, 2002.

Goossens HH, Van Opstal AJ. Blink-perturbed saccades in monkey. II. Superior colliculus activity. *J Neurophysiol* 83: 3430–3452, 2000.

Goossens HH, Van Opstal AJ. Dynamic ensemble coding of saccades in the monkey superior colliculus. *J Neurophysiol* 95: 2326–2341, 2006.

Groh JM. Converting neural signals from place codes to rate codes. *Biol Cybern* 85: 159–165, 2001.

Groh JM. Effects of initial eye position on saccades evoked by microstimulation in the primate superior colliculus: implications for models of the SC read-out process. *Front Integr Neurosci* 4: 130, 2011.

Guillaume A, Pélisson D. Gaze shifts evoked by electrical stimulation of the superior colliculus in the head-unrestrained cat. I. Effect of the locus and of the parameters of stimulation. *Eur J Neurosci* 14: 1331–1344, 2001.

Hikosaka O, Wurtz RH. Modification of saccadic eye movements by GABA-related substances. I. Effect of muscimol and bicuculline in monkey superior colliculus. *J Neurophysiol* 53: 266–291, 1985a.

Hikosaka O, Wurtz RH. Modification of saccadic eye movements by GABA-related substances. II. Effects of muscimol in monkey substantia nigra pars reticulata. *J Neurophysiol* 53: 292–308, 1985b.

Histed M, Bonin V, Reid R. Direct activation of sparse, distributed populations of cortical neurons by electrical microstimulation. *Neuron* 63: 508–522, 2009.

Katnani HA, Gandhi NJ. Analysis of current and frequency stimulation permutations in the superior colliculus. *Soc Neurosci Abstr* 77.9, 2010.

Katnani HA, Gandhi NJ. Order of operations for decoding superior colliculus activity for saccade generation. *J Neurophysiol* 106: 1250–1259, 2011.

Kim B, Basso MA. A probabilistic strategy for understanding action selection. *J Neurosci* 30: 2340–2355, 2010.

Lee C, Rohrer WH, Sparks DL. Population coding of saccadic eye movements by neurons in the superior colliculus. *Nature* 332: 357–360, 1988.

Lee P, Hall WC. An in vitro study of horizontal connections in the intermediate layer of the superior colliculus. *J Neurosci* 26: 4763–4768, 2006.

McIlwain JT. Lateral spread of neural excitation during microstimulation in intermediate gray layer of cat's superior colliculus. *J Neurophysiol* 47: 167–178, 1982.

McPeek RM, Han JH, Keller EL. Competition between saccade goals in the superior colliculus produces saccade curvature. *J Neurophysiol* 89: 2577–2590, 2003.

McPeek RM, Keller EL. Saccade target selection in the superior colliculus during a visual search task. *J Neurophysiol* 88: 2019–2034, 2002.

Meredith MA, Ramoa AS. Intrinsic circuitry of the superior colliculus: pharmacophysiological identification of horizontally oriented inhibitory interneurons. *J Neurophysiol* 79: 1597–1602, 1998.

Munoz DP, Istvan PJ. Lateral inhibitory interactions in the intermediate layers of the monkey superior colliculus. *J Neurophysiol* 79: 1193–1209, 1998.

Mysore S, Knudsen E. The role of a midbrain network in competitive stimulus selection. *Curr Opin Neurobiol* 21: 653–660, 2011.

Nichols MJ, Sparks DL. Component stretching during oblique stimulation-evoked saccades: the role of the superior colliculus. *J Neurophysiol* 76: 582–600, 1996.

Noto CT, Gnadt JW. Saccade trajectories evoked by sequential and colliding stimulation of the monkey superior colliculus. *Brain Res* 1295: 99–118, 2009.

Ottes FP, Van Gisbergen JA, Eggermont JJ. Visuomotor fields of the superior colliculus: a quantitative model. *Vision Res* 26: 857–873, 1986.

Pettit DL, Helms MC, Lee P, Augustine GJ, Hall WC. Local excitatory circuits in the intermediate gray layer of the superior colliculus. *J Neurophysiol* 81: 1424–1427, 1999.

Port NL, Wurtz RH. Sequential activity of simultaneously recorded neurons in the superior colliculus during curved saccades. *J Neurophysiol* 90: 1887–1903, 2003.

Ranck JB Jr. Which elements are excited in electrical stimulation of mammalian central nervous system: a review. *Brain Res* 98: 417–440, 1975.

Robinson DA. Eye movements evoked by collicular stimulation in the alert monkey. *Vision Res* 12: 1795–1808, 1972.

Robinson DA. A method for measuring eye movement using a scleral search coil in a magnetic field. *IEEE Trans Biomed Eng* 10: 137–145, 1963.

Sparks DL, Holland R, Guthrie BL. Size and distribution of movement fields in the monkey superior colliculus. *Brain Res* 113: 21–34, 1976.

Sparks DL, Mays LE. Signal transformations required for the generation of saccadic eye movements. *Annu Rev Neurosci* 13: 309–336, 1990.

Sparks DL, Mays LE. Spatial localization of saccade targets. I. Compensation for stimulation-induced perturbations in eye position. *J Neurophysiol* 49: 45–63, 1983.

Stanford TR, Freedman EG, Sparks DL. Site and parameters of microstimulation: evidence for independent effects on the properties of saccades evoked from the primate superior colliculus. *J Neurophysiol* 76: 3360–3381, 1996.

Stoney SD Jr, Thompson WD, Asanuma H. Excitation of pyramidal tract cells by intracortical microstimulation: effective extent of stimulating current. *J Neurophysiol* 31: 659–669, 1968.

Tehovnik EJ. Electrical stimulation of neural tissue to evoke behavioral responses. *J Neurosci Methods* 65: 1–17, 1996.

Van Gisbergen JA, Van Opstal AJ, Tax AA. Collicular ensemble coding of saccades based on vector summation. *Neuroscience* 21: 541–555, 1987.

Van Opstal A, Goossens H. Linear ensemble-coding in midbrain superior colliculus specifies the saccade kinematics. *Biol Cybern* 98: 561–577, 2008.

Van Opstal AJ, Van Gisbergen JA. Role of monkey superior colliculus in saccade averaging. *Exp Brain Res* 79: 143–149, 1990.

Van Opstal AJ, Van Gisbergen JA. Skewness of saccadic velocity profiles: a unifying parameter for normal and slow saccades. *Vision Res* 27: 731–745, 1987.

Van Opstal AJ, Van Gisbergen JA, Smit AC. Comparison of saccades evoked by visual stimulation and collicular electrical stimulation in the alert monkey. *Exp Brain Res* 79: 299–312, 1990.

Walton MMG, Sparks DL, Gandhi NJ. Simulations of saccade curvature by models that place superior colliculus upstream from the local feedback loop. *J Neurophysiol* 93: 2354–2358, 2005.

Yoshida K, Iwamoto Y, Chimoto S, Shimazu H. Saccade-related inhibitory input to pontine omnipause neurons: an intracellular study in alert cats. *J Neurophysiol* 82: 1198–1208, 1999.